

Review Article

Free Span Analysis for Submarine Pipelines

Mehrdad Mohaddes Pour ¹, Seyed Sina Razavi Taheri,¹ and Amirhosein moniri abyaneh²

¹Faculty of Civil Engineering, University of Tehran, Tehran, Iran

²Faculty of Civil Engineering, Amirkabir University of Technology, Tehran, Iran

Correspondence should be addressed to Mehrdad Mohaddes Pour; m.mohaddespour@ut.ac.ir

Received 19 June 2021; Accepted 21 July 2021; Published 5 August 2021

Academic Editor: S. Mahdi S. Kolbadi

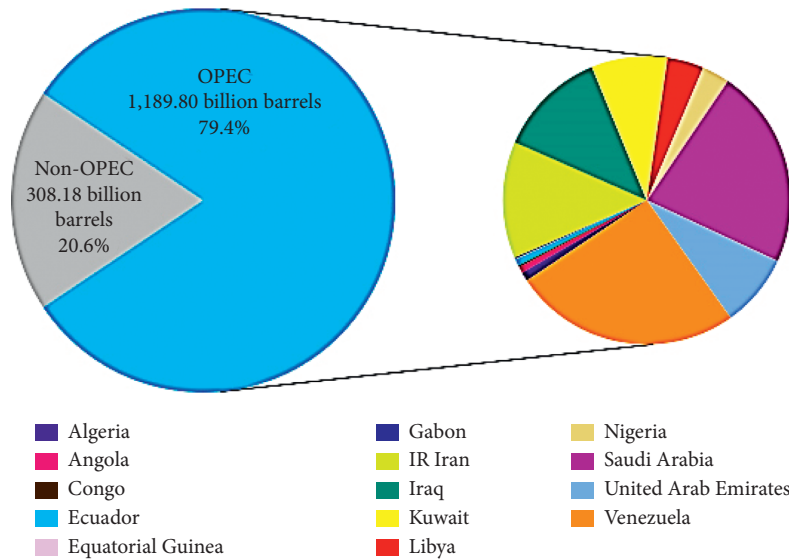
Copyright © 2021 Mehrdad Mohaddes Pour et al. This is an open access article distributed under the Creative Commons Attribution License, which permits unrestricted use, distribution, and reproduction in any medium, provided the original work is properly cited.

Pipelines are one of the most important and key elements that align with transferring hydrocarbon products in coastal and offshore industries which are exposed at various risks during their servicing. In this project, we are studding and describing free spanning of marine pipeline based on DNVGL-RP-F-105 regulation applying the finite element method by Abaqus software. For modeling, case studies of Gorze to Kish oil pipeline have been used. In order to provide and study the integrity of the structure against fatigue, the exact place as well as the free span length using software under environmental loading based on DNVGL-RP-F205 has been determined. Since based on DNVGL-TS-F101 free span causes local buckling, fatigue, and pipe burst then given to the servicing as well as environmental conditions, pipe condition has been monitored. Finally, using sensitivity analysis, the effect of different soil classes, elasticity module, and temperature on the pipe condition has been studied. At the end, the question if it is allowed to use a cross model for bed has been answered in previous studies.

1. Introduction

Marine pipelines are used to align with transferring gas and oil products under the sea water. Increasing demand for oil and gas with expansion of industry and, consequently, deficiency of fossil sources of energy causes offshore projects to develop dramatically to discover, extraction, and hydrocarbon transfer. The first marine pipe line to transfer fuel for the Second World War was the PULTO project which was installed using a ship and a large spool, a small diameter pipe between Europe and Britain with a gun. The first offshore pipeline was installed in the Gulf of Mexico. Afterwards, with the development of offshore industry, pipelining in various regions including the North Sea, Gulf of Mexico, Mediterranean, Australia, Southeast of Asia, Persian Gulf, and Latin America was conducted [1]. Iran as one of the countries which is located at this sensitive region has great, in Asalouyeh gas field, Oman Sea, etc., oil productions that this issue can be understood well, Figure 1.

1.1. Literature Review. Around 7000 years before, the Chinese invented a pipeline from Bambuseae to transfer the water and Assyrians, Egyptians, Greeks, and Romans made pipes from baked clay and created pipelines by placing clay water pipes beside each other [1]. The first pipeline to transfer oil materials was established after digging the first well in America in 1874 (1253 SH). The length of this pipe was 10 km, and it was made of wood and transferred Pennsylvania state reservoirs to Petersburg industrial city [2]. Four years later, pipelines made of iron with 5 cm diameter and with 8 km length were constructed in America that carried 250 tons of oil a day using a steam pump. In 1878 (1257 SH), a 160 km pipeline was constructed too which passed through the Allegheny Mountain Range in America [3]. The first oil pipelines in the world were established to transfer the oil from extracted underground reservoirs to the refineries and further and the advantage of transferring using pipelines over other devices was revealed, and the pipeline entered the area of oil product transferring operation as well [4]. Natural frequency of free span is considered



OPEC proven crude oil reserves, at end 2018 (billion barrels, OPEC share)

Venezuela	302.81	25.5%	Kuwait	101.50	8.5%	Algeria	12.20	1.0%	Gabon	2.00	0.2%
Saudi Arabia	267.03	22.4%	UAE	97.80	8.2%	Ecuador	8.27	0.7%	Equatorial Guinea	1.10	0.1%
IR Iran	155.60	13.1%	Libya	48.36	4.1%	Angola	8.16	0.7%			
Iraq	145.02	12.2%	Nigeria	36.97	3.1%	Congo	2.98	0.3%			

FIGURE 1: OPEC share of the world crude oil reserve, 2018 (OPEC Annual Statistical Bulletin, 2019).

as a key parameter in free span. Determining the natural frequency of a marine pipeline at the free span state and effective parameters on it were studied by Yaghubi, Maza-heri, and Jabari [5] in 2011.

In this study, the natural frequency of the marine pipeline was calculated analytically and the effect of pipe mass, axial force, soil type, and friction between the pipe and soil parameters was assessed at different support conditions so that the effect of each parameter on the natural frequency of free span in different lengths and soils can be seen [6]. Results indicated that the natural frequency of free span of marine pipelines depends on so many factors such as boundary conditions of the supports, axial force, internal pressure, and bed soil that, if ignored, can lead to errors in calculations of the natural frequency and, consequently, amplitude of vibration, tension cycles, and fatigue damages [7]. The fatigue of the free spin of the marine pipelines under repetitive loads is one of the most important failure states in the free span of the marine pipelines, which should be investigated. For this purpose and to simplify the static analysis of the fatigue phenomenon resulting from free span in marine pipelines, the DNV-RP-F-105 regulation categorizes pipeline behavior into four categories based on the ratio of free span length to the diameter of the pipeline. Amir-Heidari et al. [8] have studied fatigue analysis results from free span of the marine pipelines of the South Pars gas field. In this study, theoretical models of force have not been considered. Meanwhile, using finite element modeling and taking into account a linear model for soil behavior, soil behavior against vortex flow has been predicated [9].

2. Materials and Methods

2.1. Designing a Marine Pipeline. To ensure the maximum level of safety for the pipeline, pipe parameters should be assessed and selected carefully [10]. Various methods for design and analysis are studied in this article. Meanwhile, selecting pipeline parameters as the results of various analysis are studied [11]. Although some of these elements may not fit in, the installation includes most applications such as measurement of flow characteristics, hydrodynamic forces, internal pressure, pipe oscillation resulting from the vortex, soil-pipeline stability, buckling of the pipeline, the effect of big movements of the soil, faults, the existence of obstacles at the bed, and unevenness that may cause span at the pipeline [12]. The first step toward the construction of a structure is the design, which is described in some references as the foundation of the building. Generally, designing methods of marine structure are based on several principles [13].

This method is based on the determination of fixed decreasing and increasing coefficients, which provide a fix coefficient for the load and resistant amounts taking into consideration the contingency of maximum critical environmental conditions [14]. One of the most important achievements of this method is the optimization of the initial designing cost. This method is based on possible changes of the loads and material properties [15]. The limit state method considers uncertainties related to the loads and material properties; therefore, it uses relative safety factors to gain loads and stresses of the design [16]. The limit state

method is based on estimations. This method is unlike the allowable stress design in which it is assumed that the loads, safety factors, and stress of the materials are exactly specified [17]. In the limit state method, relative safety factors are obtained using statistics and probability. Safety factors are different for different mixtures of loads, and then, designing is carried out with a more logical and scientific method. If we want to state the designing process of a marine pipeline, we can list the stages as in Figure 2.

2.2. Hydrodynamic Loads. It is a process which is generated from the intervention of a pipeline with the environment [19]. First, they are generated from the intervention of the wave with the flow and include gravitational forces such as net weight, buoyancy, and hydrostatic pressure [20]. Other environmental loads include the pressure of the soil and other natural activities such as ambient temperature [21]. The pipeline which is laid down at the seabed is affected by the loads resulting from the waves and sea flows (Figure 3) [23]. In some regions, these forces work laterally or as a lift. In this situation, designing according to the most regulations, a safety factor should be take into consideration too.

$$\gamma(F_D - F_I) \leq \mu_L (W_{\text{sub}} - F_L), \quad (1)$$

where γ = safety factor (usually higher than 1.1), F_D = drag force, F_I = inertia force, μ_L = friction coefficient of the bed, and W_{sub} = submerged weight.

Wave and flow data to calculate input forces should be indicative of the most critical state. For example, to design a pipeline during its lifetime, waves with return period of 100 years is used [24]. Return periods of 1 and 5 years are used to analyze at the installation state in which no pipe has been placed under the operation [25]. The friction coefficient can be ranged from 0.1 to 1 depending on the material on the pipe and soil of the seabed [26].

2.3. Fatigue Failure Criterion. Breakdowns resulting from fatigue are a major concern in engineering design [27]. Economic costs of the failure and its prevention are very high, and it is taken into consideration that nearly 80% of these costs include the situations that cyclic loading and fatigue are at least one contributing factor [28]. Therefore, the annual cost of material fatigue to the U.S economy is nearly 3% of the GDP and the same percentage is anticipated for other industrial countries. Currently, three methods exist for assessing fatigue, which have been provided in Figure 4 [29].

The S-N Curve is an appropriate and effective method to analyse fatigue of the pipeline in which S-N data are usually determined with a fatigue test. According to DNV-RP-C203, the S-N initial design curve can be given as follows [30, 31]:

$$\log N = \log \bar{a} - m \log \Delta \sigma. \quad (2)$$

The S-N curve is an appropriate and effective method to analyse fatigue of the pipeline in which S-N data are usually determined using a fatigue test. According to DNV-RP-

C203, the S-N initial design curve can be provided as follows [3, 32, 33]:

$$\log \bar{a} = \log a - 2s, \quad (3)$$

where N is the number of the anticipated cycles of failure, $\Delta \sigma$ is the stress amplitude, m is the negative reverse slope of the S-N curve, and $\log a$ is the axis separator of the $\log N$ axis by the S-N curve which is given as follows [34]:

$$D_{\text{fat_life}} = \sum_{i=1}^k \frac{n_i}{N_i} = \frac{1}{a} \sum_{i=1}^k n_i (\Delta \sigma_i)^m, \quad (4)$$

where a is fixed which is related to the average of the S-N curve and standard deviation of the $\log N$. Meanwhile, fatigue lifetime can be assumed based on the S-N curve under cumulative linear breakdown using the Palmgren-Miner theory [35]:

$$T_{\text{fat_life}} = \frac{\eta}{D_{\text{fat_life}}}. \quad (5)$$

Here, $D_{\text{fat_life}}$ is cumulative linear breakdown, a is the meeting place of the S-N design curve with $\log N$, m is the negative reverse slope of the S-N curve, K is the number of the stress blocks, n_i is the number if the stress cycles in the tension block i , and N_i is the number of the failure cycles at the range of fixed stress $\Delta \sigma$. Anticipating fatigue life for the marine pipeline can be obtained using cumulative breakdown resulting from $D_{\text{fat_life}}$ and η coefficient [26].

2.4. Formulas of the DNV Regulation. DNV-RP-F-105 regulation has provided a relationship in order to validate the finite element model [30]; each of the parameters of the abovementioned relationship is defined as follows [36]:

$$f_1 = C_1 \sqrt{1 + \text{CSF}} \sqrt{\frac{EI}{m_e L_{\text{eff}}^4} \left(1 + \frac{S_{\text{eff}}}{P_{\text{cr}}} + C_3 \left(\frac{\delta}{D} \right)^2 \right)}, \quad (6)$$

where C_1 , C_3 = coefficient of boundary conditions, E = steel's modulus of elasticity, I = steel's moment of inertia, SF = stiffness correction factor of the concrete, L_{eff} = effective free span length, m_e = effective mass, D = external diameter of the pipe, $P_{\text{cr}} = (1 + \text{CSF}) C_2 \pi^2 EI / L_{\text{eff}}^2$, Δ = static deformation, and S_{eff} = effective axial force.

C_1 , C_2 , and C_3 are determined given to the boundary condition of the model which can be determined based on Table 1.

3. Analysis of Results

3.1. Validation. For validation, numerical modeling and its comparison with DNV regulation have been used. In the DNVGL-RP-F-105 reregulation, it is pointed out that, for validation, the frequency of the numerical model should be compared with the frequency obtained from the formulas [37]. In this section, modeling has been conducted both in two and three dimension and frequency analysis has been provided in both two- and three-dimensional modeling at

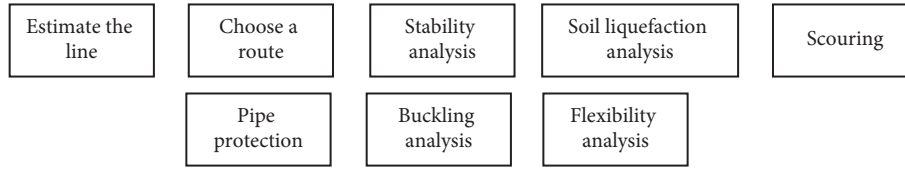


FIGURE 2: Steps of designing a submarine pipe [18].

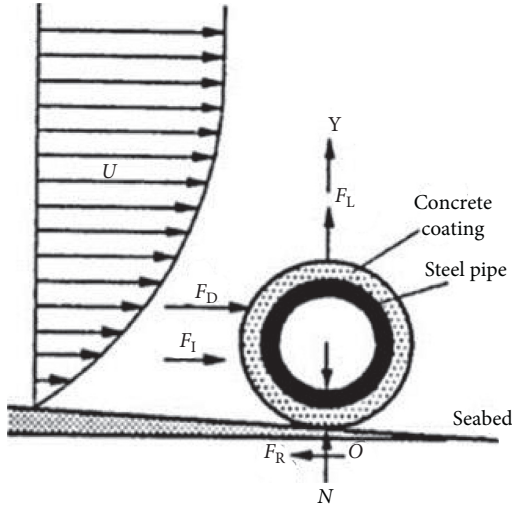


FIGURE 3: Forces on the pipe [22].

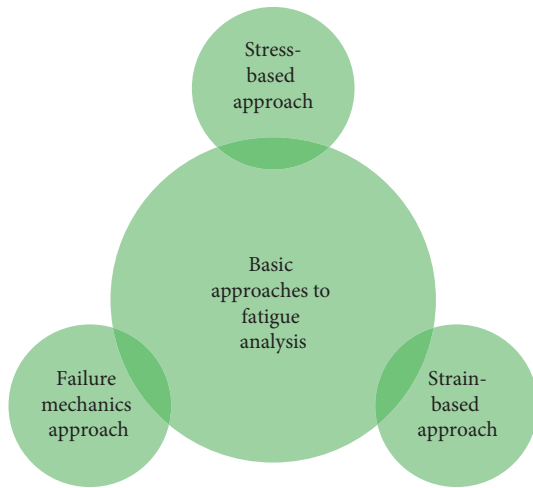


FIGURE 4: Basic approaches to fatigue analysis and design [26].

TABLE 1: Boundary condition coefficients [21].

	Pinned-pinned	Fixed-fixed	Single span on the seabed
C_1	1.57	3.56	3.56
C_2	1.0	4.0	4.0
C_3	0.8	0.2	0.4
C_6	5/384	1/384	1/384

the end of this section. In this section, two- and three-dimensional modeling have been provided, respectively, for the pipe with a free span length of 50 m and 40 m and depth

of 2 m according to the following stages step by step (Figure 5). In this section, in the three-dimensional modeling, a pipe with the length of 150 m has been placed on the soil bed (Figure 6). In order to allocate materials to the free span pipe as well as soil bed, steel with $2.07 \text{ E}6$ modulus of elasticity has been used and the soil bed has been considered as the compact sand according to the DNVGL-RP-F-105 regulation. Pipe and soil specifications have been provided at Table 2.

For interaction of the soil and pipe, the definition of the friction coefficient has been used [39]. The assumed friction coefficient for the pipe and soil bed has been considered as 0.3. Boundary conditions of the soil bed, which have been modeled two and three dimensionally, have been closed at the X- and Y-direction, and the free span pipe has been defined as one tail joint and one tail roller at both ends [40]. To analyze the frequency of the free span pipe, a fine mesh is used for meshing in places where the pipe contacts with the soil and moderate meshing is used in the free span places.

Meshing at the places where the pipe and soil bed contact each other has been considered as the pipe diameter (0.8 m). In Figure 5, meshing is provided two and three dimensionally. In Figure 6, meshing is presented in a three-dimensional and two-dimensional mode. According to the DNV regulation, if the difference in the results obtained from regulation formulas and numerical analysis is placed at the range of $\pm 5\%$, then finite-element analysis is acceptable. In Table 3, numerical analysis conducted by Abaqus finite-element software and the regulation formulas are provided. From Table 3 it is specified that results from numerical analysis and regulation formulas are at the range of $\pm 5\%$; then, modeling is correct and reliable.

3.2. Numerical Analysis and Discussion. After determination of critical free span, local modeling is conducted [42]. For closer studying and for the sake of parameter importance, the model should be modeled three dimensionally with the soil bed as solid and the pipe as shell (stress change is not important in the pipe thickness) [43]. Free span length according to the output of the previous section is 100 m, and maximum free span depth is 1.7 m; modeling has been conducted using these numbers [44]. According to the first chapter, soil specifications of the place as well as required models for the model in an operational state have been used from the report of the study. Hydrodynamic loads according to the first flow regime in Section 2 should be calculated based on equation (7) and Table 4. We have

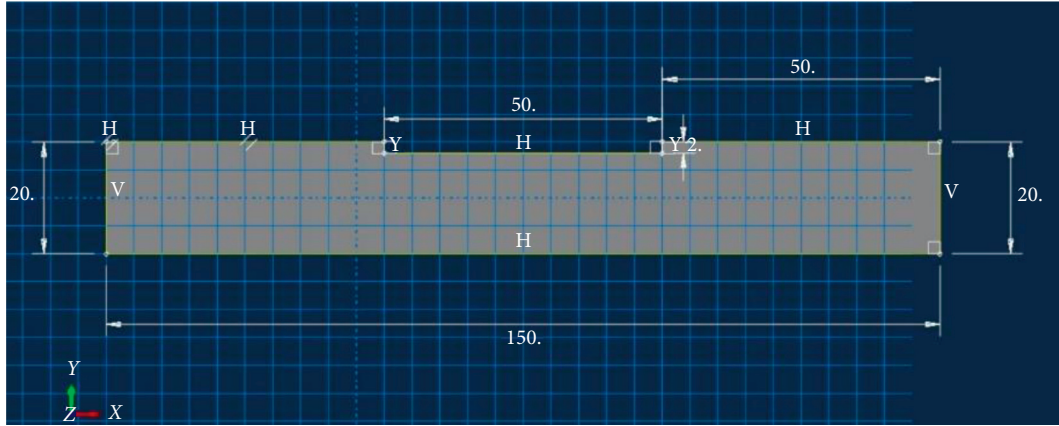


FIGURE 5: Size and dimensions of the soil and pipe bed for the three-dimensional mode.

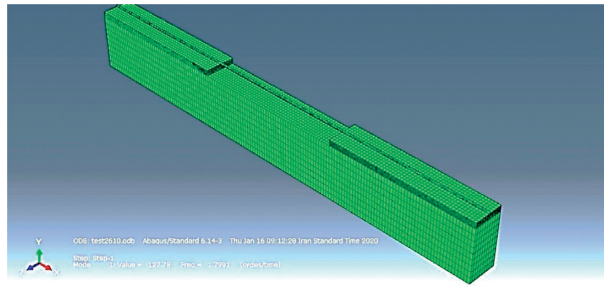


FIGURE 6: Display of the bed soil mesh and free opening pipe for three-dimensional modeling.

TABLE 2: Pipe and bed soil specifications [38].

Poisson's ratio	Modulus of elasticity (MPa)	Density (kg/m ³)	Type of materials
35/0	207000	1300	Soil bed
3/0	20	7850	Pipe

TABLE 3: Frequency analysis with the results of numerical analysis and code formulas [41].

Regulation formulas (1/s)	Frequency of numerical analysis (1/s)	No.
2.798	2.628	2D
1.801	1.199	3D

TABLE 4: The relationship parameters.

γ_m	γ_{sc}	M_{sd}	S_{sd}	α_c	$M_p(t_2)$	$S_p(t_2)$	α_p
1.15	1.308	1600 (N-M)	16041515.7 (N)	1.035	5720 (N-M)	22903020.1 (N)	0.5

$$0.8 < \alpha = \frac{U_C}{U_c + U_w} \tag{7}$$

In Shabani's article [17], it is specified that the alpha range is higher than 0.8 for the undersea pipes always in the Persian Gulf. Therefore, hydrodynamic loads only result from the flow rate. After analyzing finite element by the software, the output of the maximum stress and displacement is provided as follows. Now, the analysis provided in Section 2 based on the regulation should be conducted on the free span.

3.3. *Elasticity Modulus of the Soil Bed.* In this section, the modulus of elasticity has been considered to be 15, 20, 25, and 55 MPa. Furthermore, sampling of the conducted modeling and the effect of bed soil modulus of elasticity on the output has been seen. It can be clearly understood from the picture that final result (vertical displacement) has not been affected by the modulus of elasticity but the main point is the slope of the graphs that this slope is lower for soil with lower modulus or it can be better said that the time arrival to this displacement occurs later, and this analysis is correct when the higher amount of clay is considered. The

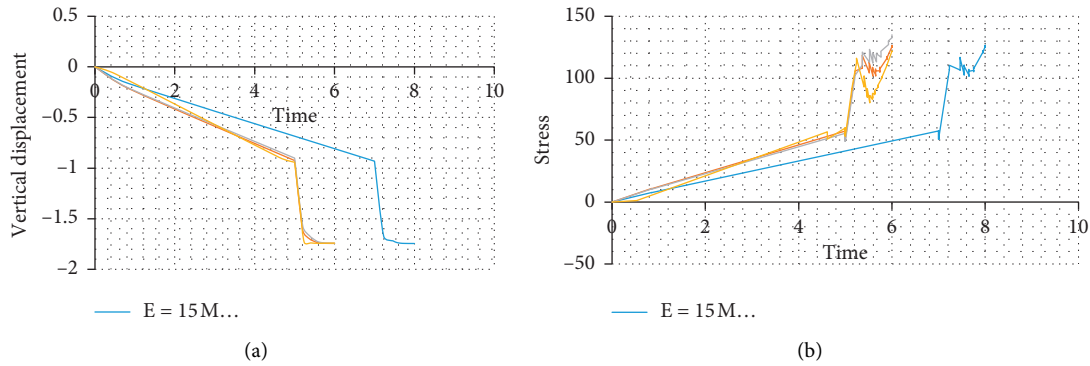


FIGURE 7: Display of time diagram-vertical displacement and Von Mises of a pipe with different moduli of elasticity of bed soil.

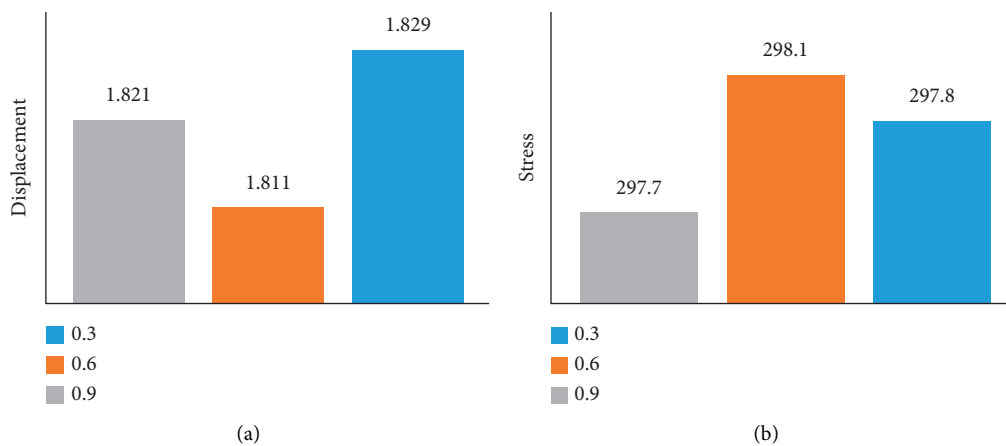


FIGURE 8: Pipe displacement and Von Mises for different coefficients of friction.

point which is proposed in the meantime is its effect on the pipe behavior against imposed loads from the environment. If, by assuming the correctness of Hooke's law (because the stresses are lower than yield stress), we consider that the relationship between the stress and displacement is direct, then the time that the stress reaches t its maximum level is higher in the soils with lower modulus, and this is better for the health of the structure. On the other word, by increasing the available opportunity for doing the activity without worry about the condition of the fatigue of the pipe, cost of missed opportunity can be decreased and the costs resulting from servicing at other places can be investigated to increase profitability to the employer. Alternatively, it can be to answer this basic question whether it is correct to use a cross model in studies such as in [17, 28]. Given the abovementioned graph, it can be said that by considering the bed as a cross, there will be no significant difference in the answers. Then, this amount is better not only from scientific but also from applied perspective to use a cross bed. As it can be seen in the figure, as the soil hardens, the maximum stress condition worsens

because the fatigue life is a reverse function of the stress [45]. Then, the situation is worse in the harder than fine soils (Figure 7).

3.4. Studying the Friction Coefficient of the Soil with the Pipe. To study the friction coefficient of the soil bed with the pipe, the friction coefficients were considered 0.3, 0.6, and 0.9. One can understand from Figure 8 that, for smaller coefficients, greater oscillation range will be obtained, which will be obvious by taking into account friction as the only factor against the pipe vibrations. Contrary to what was seen above, it was expected that, for finer soils, more stress can be obtained for the greater displacement amplitude, but the highest stress was gained in the soil with 0.6 friction coefficient, which, of course, is much smaller than the stress with 0.9 friction coefficient (nearly 0.067159%). But, if we assess the general condition of he stresses relative to each other, percentage difference is nearly lower than 0.15 in three models. On the other hand, it can be understood that, in the present model, this factor does not affect significantly the

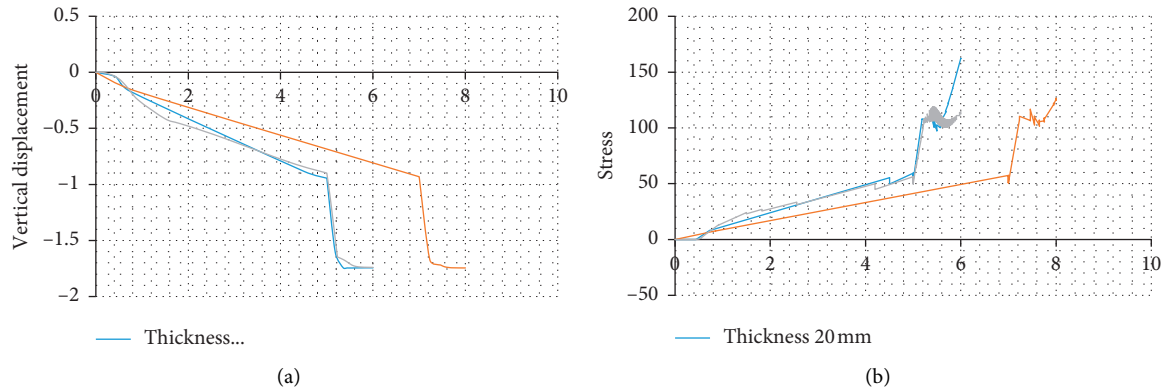


FIGURE 9: Response of vertical displacement and Von Mises of 20, 25, and 30 mm thick pipes.

fatigue life that it is expected to be due to the smallness of tension and the need to repeat a lot to achieve fatigue. If the amount of stress (loadings) was very high, this condition would have been completely different.

3.5. Studying the Thickness of the Pipe. In this study, the thickness of the pipe was considered as 25.4 mm and pipes with 30 mm and 20 mm thicknesses have been considered as well to study the effect of increasing and decreasing the thickness on the free span stress. According to Figure 9 and comparison of the pipes with 20, 25, and 30 mm thicknesses, it was specified that increasing the thickness of the pipe does not change the amount of vertical displacement of the pipe significantly. Another point which can be understood from the abovementioned graph is the arrival time to the given displacement that, in 20 and 30 mm diameters, no specific change is observed but in the mode of 25 mm diameter, this amount increases to 16.67%. According to Figure 9 and comparison of the pipes with 20, 25, and 30 mm thicknesses, it was specified that by increasing the thickness of the pipe, consequently, the total weight of the pipe increases and the amount of stress decreases with the increase of thickness.

4. Conclusions

In the present study, we first reviewed previous activities in the free span field and further proposed the method by the regulation which was used to study the health status of the Gorze to Kish pipeline against free span. To determine and identify free spans and measure the length of each span, total pipeline was modeled in the Abaqus software environment and the sizes of three spans have been obtained. As it was required that trivial stresses be studied, trivial modeling for each span has been conducted by taking different boundary conditions into account. Meanwhile, the proposed criterion of the regulation has been used for validation which is the same as the natural frequency of oscillations. Finally using one-way sensitivity analysis, the effect of soil modulus of elasticity, coefficient of friction, span diameter, and operational temperature has been studied. According to the obtained results, pipe fatigue life (without taking into account corrosion conditions, collision, erosion or landslide, and so

on) was much higher than the required amount. Meanwhile, the safety status of the pipe against other accidents was at the safe margin of the regulation. Meanwhile, results indicated that as soil hardens, displacement will not change significantly but required time to arrive at the final point will be lower that confirms assuming the bed model as a cross in previous studies and correctness of this assumption. But, these changes of Young's modulus do not have any influence on the obtained stress and cannot practically affect the fatigue life. Naturally, as the soil becomes finer (lack of friction between the soil and the pipe), the amplitude of the displacements increases, but this amount of displacement does not affect the maximum amount of the stress. Therefore, significance index of this factor on the fatigue life is nearly zero. Another point that has been obtained from this study is the passiveness of the pipe thickness. On the other word, by increasing the thickness of the pipe, generated stress in the pipe reduces. Therefore, this can be used as a factor by taking the economy situation into account in the regions where predictive operations such as earth filling, using concrete plates or artificial support, are impossible. Another issue that is seen in this study is that operational temperature does not have any influence on the amplitude of the displacements but increases the stress in the pipes.

Data Availability

Requests for access to these data should be made to the corresponding author at m.mohaddespour@ut.ac.ir.

Conflicts of Interest

The authors declare no conflicts of interest regarding the publication of this paper.

References

- [1] S. Shadpoor, A. Pirouzi, H. Hamze, and D. Mazaheri, "Determination of Bodenstein number and axial dispersion of a triangular external loop airlift reactor," *Chemical Engineering Research and Design*, vol. 165, pp. 61–68, 2021.
- [2] DNV, *Dnvgl-Ts-F101: Submarine Pipeline Systems*, DNV, Bærum, Norway, 2017.

- [3] R. E. Hobs, "Influence of Structural Boundary Conditions on Pipeline Free Span Dynamics," in *Proceedings of the International Offshore Mechanics and Arctic Engineering*, Tokyo, Japan, 1986.
- [4] O. Fyrileiv and K. Mørk, "Structural response of pipeline free spans based on beam theory," in *Proceedings of the 22nd International Conference on Offshore Mechanical and Arctic Engineering, OMAE*, Oslo, Norway, June 2002.
- [5] Abaqus Version, 6.13 documentation collection, Dassault Systèmes, Vélizy-Villacoublay, France, 2013.
- [6] N. Fyrileiv, M. Chezhian, K. J. Mørk, K. Arnesen, and T. F. G. Søreide, "New Free Span Design Procedure for Deepwater Pipelines," in *Proceedings of the 16th Deep Offshore Technology (International Conference & Exhibition)*, New Orleans, LA, USA., 2004.
- [7] X. U. Jishang, L. I. Guangxue, J. J. Horrillo, Y. Rongmin, and C. A. O. Lihua, "Calculation of maximum allowable free span length and safety assessment of the DF1-1 submarine pipeline," *Journal of Ocean University of China*, vol. 9, no. 1, pp. 1–10, 2010.
- [8] P. Amir-heidari, M. Ebrahemzadieh, H. Farahani, and J. Khoubi, "Quantitative risk assessment in Iran's natural gas distribution network," *Open Journal of Safety Science and Technology*, vol. 4, pp. 59–72, 2014.
- [9] Y. Zhang, Z. Xiao, and J. Luo, "Fatigue crack growth investigation on offshore pipelines with three-dimensional interacting cracks," *Geoscience Frontiers*, vol. 9, no. 6, pp. 1689–1697, November 2018.
- [10] D. Yi, Z. M. Xiao, S. Idapalapati, and S. B. Kumar, "Fracture analysis of girth welded pipelines with 3D embedded cracks subjected to biaxial loading conditions," *Engineering Fracture Mechanics*, vol. 96, pp. 570–587, December 2012.
- [11] DNV, *Dnv-Rp-F105: Free Spanning Pipelines*, DNV, Bærum, Norway, 2006.
- [12] O. Hagen, K. Mørk, G. Sigurdsson, and F. G. Nielsen, "Evaluation of free spanning pipeline design in a risk based perspective," *Reliab. Pipeline Technol.* vol. 2, pp. 789–799, 2003.
- [13] F. G. Nielsen, N. Hydro, S. O. Kvarme, and R. Engineering, "VIV response of long free spanning pipelines," in *Proceedings of the International Conference on Ocean, Offshore, and Arctic Engineering (OMA)*, 2002.
- [14] Y. M. Zhang, T. K. Tan, Z. M. Xiao, W. G. Zhang, and M. Z. Ariffin, "Failure assessment on offshore girth welded pipelines due to corrosion defects," *Fatigue & Fracture of Engineering Materials & Structures*, vol. 39, no. 4, pp. 453–466, April 2016.
- [15] M. Bouatia, R. demagh, and Z. Derriche, "Structural behavior of pipelines buried in expansive soils under rainfall infiltration (Part I: transverse behavior)," *Civil Engineering Journal*, vol. 6, no. 9, pp. 1–15, 2020.
- [16] C. N. Dacuan, V. Abellana and H. A. Canseco, Mechanical properties of corroded-damaged reinforced concrete pile-supporting wharves," *Civil Engineering Journal*, vol. 6, no. 12, pp. 1–21, 2020.
- [17] S.-M. Seyed-Kolbadi, M. Safi, A. Keshmiri, S. M. S. Kolbadi, and M. Mirtaheri, "Explosive performance assessment of buried steel pipeline," *Advances in Civil Engineering*, vol. 2021, Article ID 6638867, 24 pages, 2021.
- [18] M. M. Shabani, A. Taheri, and M. Daghigh, "Reliability assessment of free spanning subsea pipeline," *Thin-Walled Structures*, vol. 120, pp. 116–123, 2017.
- [19] A. Taheri, M. Shabani, and M. Daghigh, "Investigation of the effect of local buckling and VIV fatigue on failure probability of subsea pipelines in Iranian South Pars gas field," *International Journal of Maritime Technology*, vol. 9, no. 1, pp. 23–32, Jan. 2018.
- [20] M. R. Shiravand, S. M. S. Kolbadi, N. Hassani, and S. M. S. Kolbadi, "Effect of ground motions on nonlinear seismic behavior of corroded buried gas pipeline," *American Journal of Civil Engineering*, vol. 3, no. 2-1, pp. 9–13, January 2015.
- [21] DNV, *DNV-RP-F105; Free Spanning Pipelines*, DNV, Bærum, Norway, 2nd edition, 2006.
- [22] Q. Bai and B. Yong, "1-Introduction," in *Subsea Pipeline Design, Analysis, and Installation*, pp. 5–24, Elsevier, Amsterdam, Netherlands, 2014.
- [23] M. M. Shabani, H. Shabani, N. Goudarzi, and R. Taravati, "Probabilistic modelling of free spanning pipelines considering multiple failure modes," *Engineering Failure Analysis*, vol. 106, Article ID 104169, Dec. 2019.
- [24] M. Shabani, Z. Ashoori, R. Taravat, and A. Taheri, "Reliability-Based cost optimization of corroded gas subsea pipeline in Persian gulf," 2018.
- [25] H. S. Choi, "Free spanning analysis of offshore pipelines," *Ocean Engineering*, pp. 1325–1338, Sep. 2000.
- [26] M. Drago, M. Mattioli, and R. Bruschi, "Insights on the design of free-spanning pipelines," *Philosophical Transactions of the Royal Society A*, vol. 373, 2015.
- [27] S. Li, Y. Meng, F. Ma, H. Tan, and W. Chen, "Research on the working mechanism and virtual design for a brush shape cleaning element of a sugarcane harvester," *Journal of Materials Processing Technology*, vol. 129, no. 1–3, pp. 418–422, Oct. 2002.
- [28] S. M. S. Kolbadi, N. Hassani, and M. Safi, "Numerical evaluation on improvement performance of waved connection to reduce damage on buried gas pipeline," *Shock and Vibration*, vol. 2020, Article ID 6680384, 9 pages, 2020.
- [29] Z. Chen, Y. Xiong, H. Qiu, G. Lin, and Z. Li, "Stress intensity factor-based prediction of solidification crack growth during welding of high strength steel," *Journal of Materials Processing Technology*, vol. 252, pp. 270–278, Feb. 2018.
- [30] K. Rezazadeh, L. Zhu, Y. Bai, and L. Zhang, "Fatigue analysis of multi-spanning subsea pipeline," in *Proceedings of the 29th International Conference on Ocean, Offshore and Arctic Engineering*, vol. 5, pp. 805–812, Shanghai, China, June 2010.
- [31] H. Shabani, M. M. Shabani, N. Goudarzi, and R. Taravati, "Stochastic-based quantitative risk assessment of corroded gas transmission pipelines considering multiple failure modes," *Thin-Walled Structures*, vol. 131, 2018.
- [32] American Petroleum Institute: Recommended Practice for Planning, Designing, and Constructing Fixed Offshore Platforms-Working Stress Design: Upstream Segment. API Recommended Practice 2A-WSD (RP 2A-WSD), American Petroleum Institute, 2000.
- [33] D. Leshchinsky, "ASD and LRFD of reinforced SRW with the use of software program MSEW (3.0)," *Geosynthetics*, vol. 24, no. 4, pp. 14–20, 2006.
- [34] Y. Bai and W.-L. Jin, "Chapter 1. introduction," in *Marine Structural Design*, pp. 3–18, Elsevier, Amsterdam, Netherlands, 2016.
- [35] C. E. T. Balestra, A. Y. Nakano, G. Savaris, and R. A. Medeiros-Junior, "Reinforcement corrosion risk of marine concrete structures evaluated through electrical resistivity: proposal of parameters based on field structures," *Ocean Engineering*, vol. 187, Article ID 106167, Sep. 2019.
- [36] P. Amir-heidari, M. Ebrahemzadieh, H. Farahani, and J. Khoubi, "Quantitative risk assessment in Iran's natural gas

- distribution network,” *Open Journal of Safety Science and Technology*, 2014.
- [37] F. H. van Duijne, D. van Aken, and E. G. Schouten, “Considerations in developing complete and quantified methods for risk assessment,” *Safety Science*, vol. 46, no. 2, pp. 245–254, Feb. 2008.
- [38] A. H. Mousselli, *Offshore Pipeline Design, Analysis, and Methods*, PennWell Corporation, Tulsa, OK, US, 1981.
- [39] M. Zeinoddini, G. A. R. Parke, and S. M. Sadrossadat, “Free-spanning submarine pipeline response to severe ground excitations: water-pipeline interactions,” *Journal of Pipeline Systems Engineering and Practice*, vol. 3, no. 4, pp. 135–149, Nov. 2012.
- [40] W. Zhou, “System reliability of corroding pipelines,” *International Journal of Pressure Vessels and Piping*, vol. 87, no. 10, pp. 587–595, 2010.
- [41] G. Boyun, S. Song, A. Ghalambor, and T. R. Lin, *Offshore Pipelines Design, Installation, and Maintenance*, Gulf Professional, Houston, Texas, 2nd edition, 2014.
- [42] A. Yeganeh Bakhtiary, A. Ghaheri, and R. Valipour, “Analysis of offshore pipeline allowable free span length,” *International Journal of Civil Engineering*, 2007.
- [43] J. Dong and X. D. Chen, “Local buckling analysis of free span for submarine pipeline,” *Journal of Construction Steel Research*, pp. 128–139, Elsevier Science, Amsterdam, Netherlands, Mar. 2013.
- [44] Tadbirsahelpars, “Kish gas field development project,” *Allowable span length and bottom roughness analysis report*, vol. 1, pp. 1–14, 2015.
- [45] P. Kargar, A. Osouli, and T. D. Stark, “3D analysis of 2014 Oso landslide,” *Engineering Geology*, vol. 287, no. 20, Article ID 106100, June 2021.